Carbohydrate Polymers 156 (2017) 235–243

Contents lists available at ScienceDirect

Carbohydrate Polymers

journal homepage: www.elsevier.com/locate/carbpol

Antibacterial activity and cytocompatibility of chitooligosaccharide-modified polyurethane membrane via polydopamine adhesive layer

Chuang Luo[a,b], Wenjun Liu[a,b], Binghong Luo[a,*], Jinhuan Tian[a,b], Wei Wen[a,b], Mingxian Liu[a,b], Changren Zhou[b,*]

[a] Department of Material Science and Engineering, Jinan University, Guangzhou 510632, PR China
[b] Engineering Research Center of Artificial Organs and Materials, Ministry of Education, Guangzhou 510632, PR China

ARTICLE INFO

Article history:
Received 25 June 2016
Received in revised form 4 September 2016
Accepted 13 September 2016
Available online 13 September 2016

Keywords:
Polyurethane
Dopamine
Chitooligosaccharide
Cytocompatibility
Antibacterial properties

ABSTRACT

The aim of this study was to provide a convenient surface modification method for polyurethane (PU) membrane and evaluate its influence on hydrophilicity, antibacterial activity and cell functions, which are the most important factors for wound dressings. For this purpose, chitooligosaccharide (COS) was modified onto the surface of PU membrane based on the self-polymerization of dopamine (DOPA). Surface composition, morphology, hydrophilicity and surface energy of the original and modified PU membranes were characterized. Surface roughness and hydrophilicity of the PU membrane were obviously increased by modified with polydopamine (PDOPA) and COS. Antibacterial experiment against *Escherichia coli* and *Staphylococcus aureus* indicated that antibacterial activity of PU membrane increased only slightly by modified with PDOPA, but increased significantly by further modified with COS. Cells culture results revealed that COS-functionalized PU membrane is more beneficial to the adhesion and proliferation of NIH-3T3 cells compared to the original and PDOPA-modified PU membranes.

1. Introduction

More than 80 million people were afflicted with acute and chronic dermal wounds due to surgery, burns and chronic ulcers which demand clinical care in the worldwide (Sun, Siprashvili, & Khavari, 2014). When skin has been damaged, wound dressings can protect skin from further contamination or trauma and promote wound healing. An ideal wound dressing should include some key features such as biocompatibility, preserve moisture, antibacterial activity, excellent barrier and accelerating wound healing (Xia et al., 2016). Several polymers, such as chitosan, collagen, polyurethane (PU), polyvinyl alcohol, have been widely employed as wound dressings (Hashemi Doulabi, Mirzadeh, Imani, & Samadi, 2013; Lowe et al., 2015). Among these materials, PU is a promising candidate for wound dressing due to its good biocompatibility, barrier properties and oxygen permeability (Xu, Chang, Chen, Fan, & Shi, 2013). However, some problems still remain, the hydrophilicity, antibacterial activity and cytocompatibility of PU are far from ideal, which limits the wider application of PU as a wound dressing. (Unnithan, Gnanasekaran, Sathishkumar, Lee, & Kim, 2014). In recent years, several methods such as plasma treatment (Yao, Li, Neoh, Shi, & Kang, 2008) and UV grafting (Woo et al., 2015) have been employed to modify the surface of PU, but these methods often relate to complicated procedures and a waste of time. Thus, developing a facial and convenient technique for surface modification of PU is necessary.

As the water-soluble and low molecular weight chitosan, chitooligosaccharide (COS) owns favorable biocompatibility, antibacterial activity and can stimulate the proliferation and differentiation of cells (Hu, Jou, & Yang, 2003). Being served as a part of wound dressings, COS plays an important role in antibacterial activity, accelerating wound-healing (You, Park, Ko, & Min, 2004) and inducing fibroblast cell proliferation (Chandika et al., 2015). Moreover, the biological characteristics of COS are obviously superior to those of chitosan (Muzzarelli & Muzzarelli, 2002; Yang & Yu, 2014). In a moist healing environment, COS is more effectively in accelerating wound healing than chitosan due to a relatively fast interaction between the wound and COS (Yan, Zhang, Zhang, & Ping, 2011). However, as a result of low molecular weight and high water solubility, COS cannot be directly used as a wound dressing. Thus, it is necessary to effectively immobilize COS on material surface to best take advantage of its excellent biological characteristics.

As a critical functional element in mussel adhesive protein, 3,4-dihydroxyphenethylamine (DOPA) can polymerize and stick on

* Corresponding authors.
E-mail addresses: tluobh@jnu.edu.cn (B. Luo), tcrz9@jnu.edu.cn (C. Zhou).

http://dx.doi.org/10.1016/j.carbpol.2016.09.036
0144-8617/

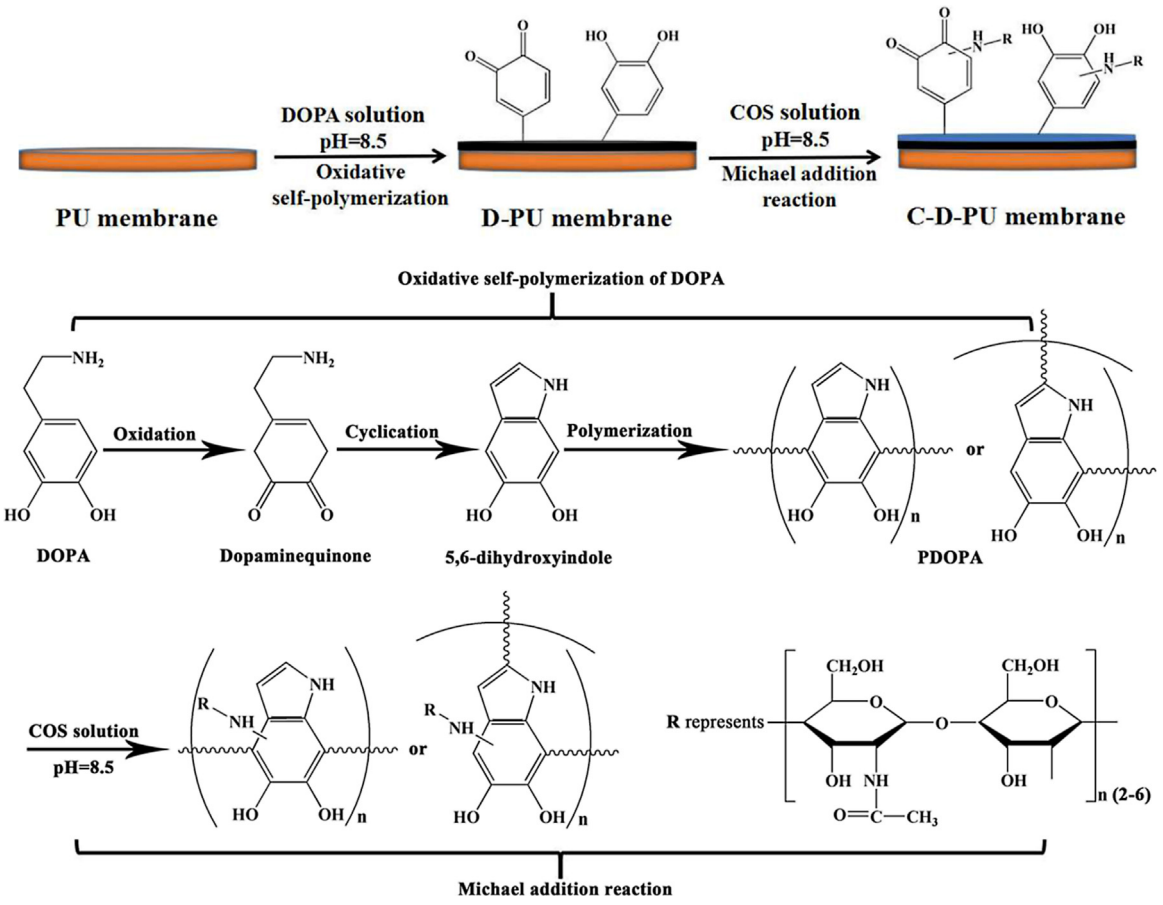

Fig. 1. Schematic diagram of the DOPA self-polymerization and subsequent COS immobilization on PU membrane.

virtually all kinds of substrates via oxidative self-polymerization (Lee, Dellatore, Miller, & Messersmith, 2007). Most importantly, the formed polydopamine (PDOPA) layer contains catechol and amine functional groups, which displays potential reactivity toward amine and thiol groups (Liu, Wang, Caro, & Huang, 2013). In this regard, a facile and effective approach for surface modification of materials has been developed based on the strong adhesion behavior and reactivity of DOPA and PDOPA layer.

In this study, in order to significantly improve the hydrophilicity, antibacterial activity and cytocompatibility of PU membrane, a thin PDOPA layer was firstly coated to the PU membrane via the self-polymerization of DOPA, which can serve as a reactive secondary platform to further immobilize COS on the surface of the membrane. Additionally, the introducing of PDOPA layer can also improve the properties of PU. Surface composition, morphology and properties of PU, PDOPA modified PU (D-PU) and COS modified D-PU (C-D-PU) membranes were investigated in detail. Furthermore, antibacterial activity and cytocompatibility of the membranes were also studied. Until recently, little has been reported on improving the properties of PU wound dressing by surface immobilization with COS through the intermediate layer of PDOPA. Thus, this study would supply a research basis for the use of the resulting C-D-PU membrane as a wound dressing.

2. Materials and methods

2.1. Materials and reagents

PU (2363-80AE) was purchased from Lubrizol Specialty Chemicals Manufacturing (Shanghai) Co. Ltd. COS (DP: 2–6) was purchased from Glyco Bio (Dalian, China). Tris (hydroxymethyl) aminomethane (Tris) and DOPA were received from Sigma-Aldrich and used as received. The *Escherichia coli* and *Staphylococcus aureus* were obtained from Colloge of Life Science (South China Agricultural University). Mouse embryonic fibroblast (NIH-3T3) cells were obtained from the Sun Yat-Sen University. All other agents are of analytical grade and used as received.

2.2. Preparation of PU, D-PU and C-D-PU membranes

PU membrane was prepared by solution casting method using THF as a solvent. A 5 *wt%* PU solution was poured on a teflon dish at room temperature. Then, PU membrane was obtained by removing the solvent thoroughly under vacuum at 40 °C.

The PU membrane was immersed into an aqueous solution of DOPA (2 g/L) in Tris (10 mM, pH = 8.5) with magnetic stirring for 24 h. After that, the membrane was taken out and cleaned with ethanol and deionized water in sequence thoroughly. Finally, D-PU membrane was obtained after being dried under vacuum at 40 °C.

The resulting D-PU membrane was immersed into 6.0 g/L COS solution with magnetic stirring at room temperature for 24 h. Then the membrane was taken out and cleaned with ethanol and deionized water in sequence thoroughly. Finally, the C-D-PU membrane was obtained after being dried under vacuum at 40 °C for 24 h.

Based on literatures reported and our previous study (Li et al., 2016; Liu et al., 2013; Liu, Ai, & Lu, 2014), the chemical reaction involves between DOPA and PU and D-PU and COS was concluded as follows (Fig. 1): A thin PDOPA film can firstly form and link to PU membrane by covalent and non-covalent bindings based on the oxidative self-polymerization of DOPA. Due to the presence of

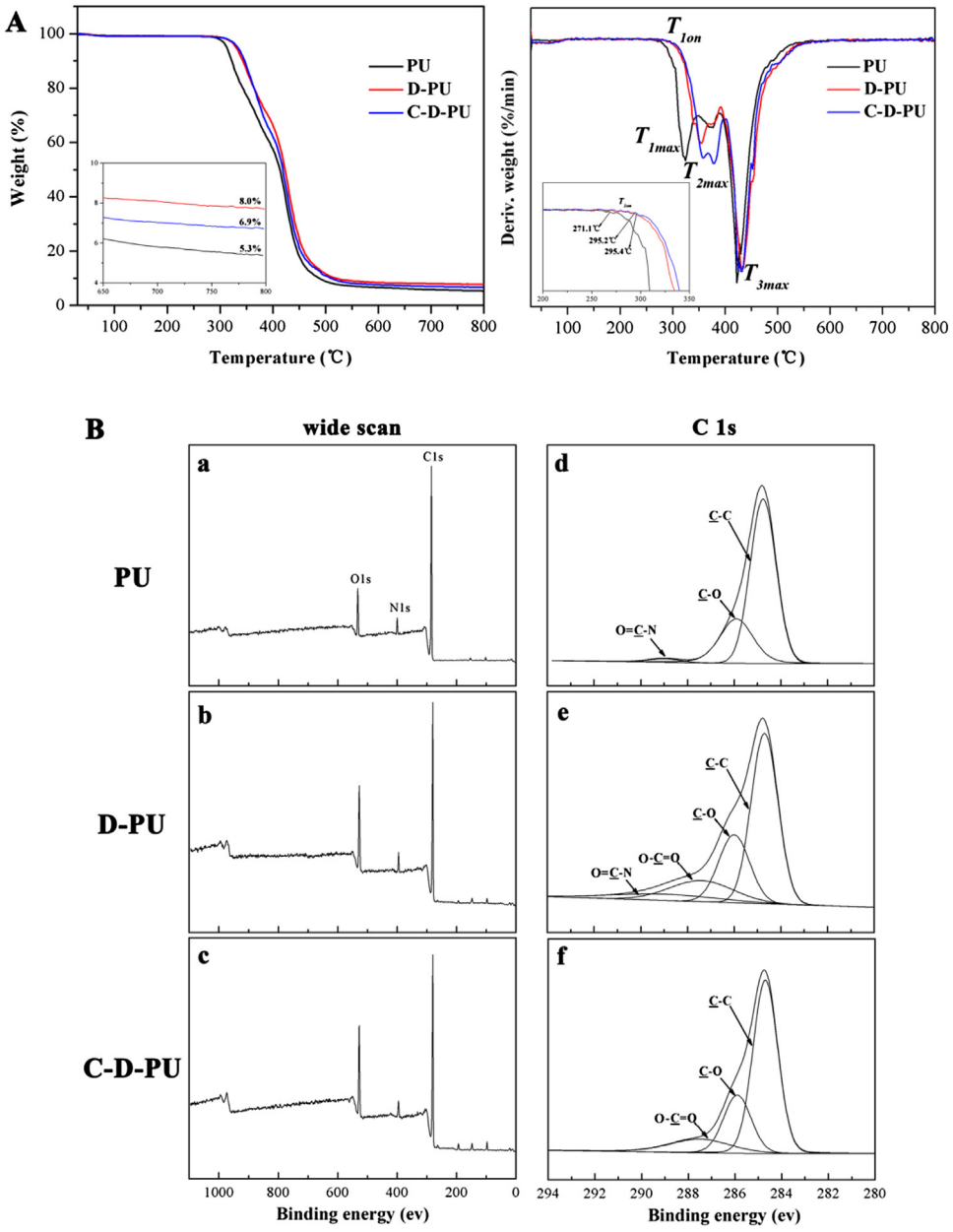

Fig. 2. The TGA and DTG curves (A), XPS wide scans and C 1 s core-level spectra (B) of the membranes.

catechol and amine functional groups in PDOPA layer, COS can be further immobilized onto the D-PU membrane surface via deprotonation and intermolecular Michael addition reaction with PDOPA layer.

2.3. Characterization

The surface chemical compositions of PU, D-PU and C-D-PU membranes were analyzed using a X-ray photoelectron spectroscopy (XPS, Thermo ESCALAB-250 System, Australia) with an aluminum (mono) Kα source (1486.6 eV). Thermogravimetric analysis (TGA) was carried out with a Netzsch-TG 209 (Germany) system under nitrogen atmosphere. Samples were heated from room temperature to 800 °C at a heating rate of 10 °C/min. Surface hydrophilicity and surface energy (SE) were measured using a goniometer (Drop Shape Analysis System, KRUSS, Germany). The zeta potential of all membranes was measured using a commercial electrokinetic analyzer (SurPASS, Anton-Paar GmbH, Austria). Surface morphologies were observed using a field emission scanning electron microscope (XL30 FESEM FEG, PHILIPS) and atomic force microscopy (AFM, Auto Probe CP Research, Thermo microscopes, USA).

2.4. Antibacterial activity testing

The antibacterial activity of the PU, D-PU and C-D-PU membranes was tested against *E. coli* (ATCC 8739) and *S. aureus* (ATCC 6538P). The bacteria were cultivated in sterilized LB medium (pH = 7.0) at 37 °C. The bacterial suspensions were obtained by the growth of each type of the bacteria in LB medium at 37 °C for 18 h. First, the membranes with dimension of 10 mm × 10 mm were immersed in 10 mL of above prepared suspension in a test tube and shaken at 150 rpm at 37 °C for 12 h. Then, 1 mL of bacterial suspension was diluted 10-fold, spread to LB agar plate and then incubated at 37 °C for 24 h. Last, for the agar plate that showed from 30 to 300 colonies, the assays were carried out by colony counting on incu-

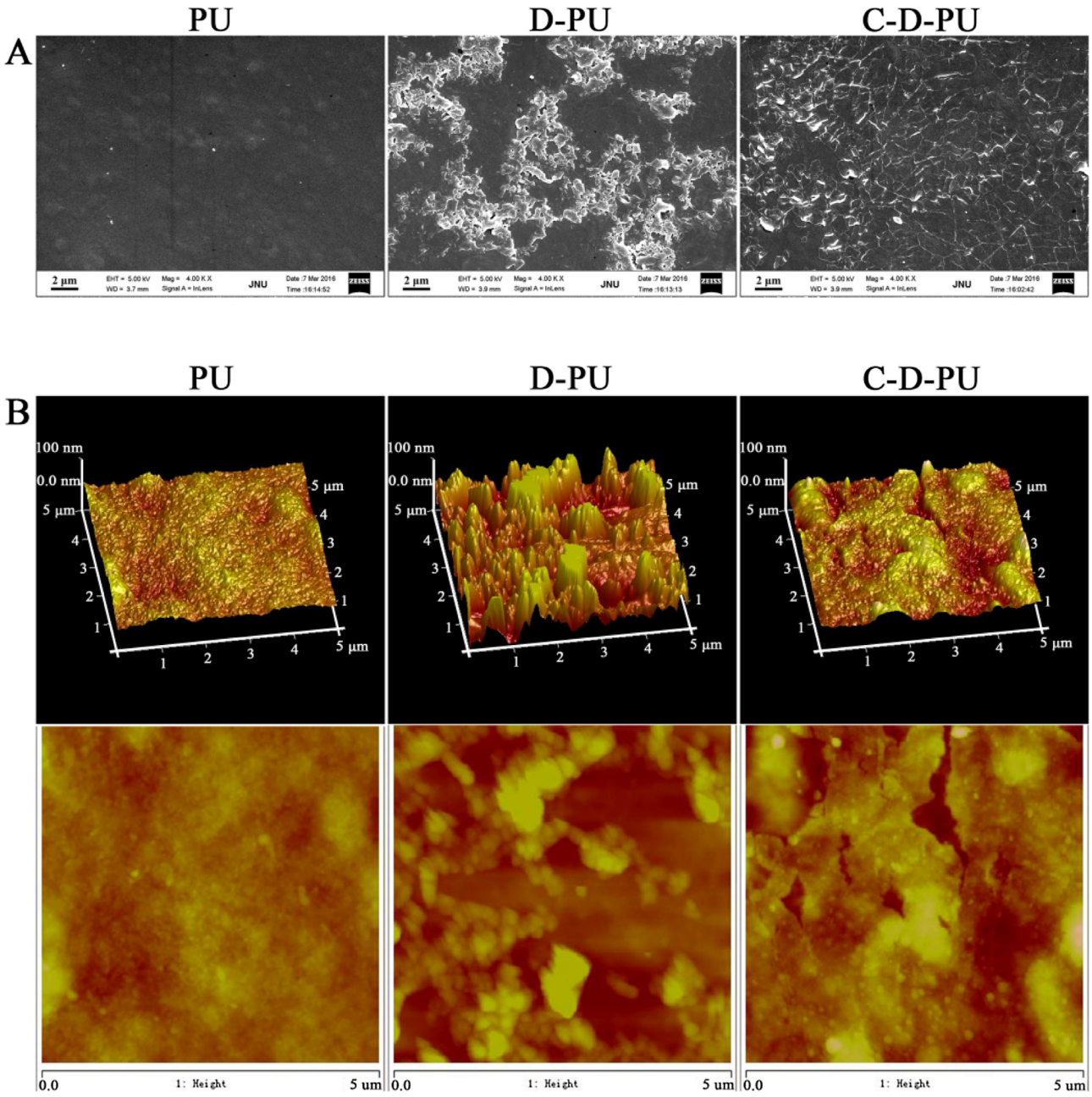

Fig. 3. FESEM (A) and AFM images (B) of the membrane surfaces.

bated agar plates. The antibacterial efficacy (ABE) was calculated using Eq. (1)

$$\mathrm{ABE} = \left[\left(V_0 - V_t\right)/V_0\right] \times 100\% \quad (1)$$

where V_0 is the number of bacterial colonies (CFU) in the control solution (PU membrane) and V_t is the number of bacterial colonies (CFU) in the test specimen solution (D-PU and C-D-PU membranes).

2.5. Cell compatibility test

The NIH-3T3 cells grow in a tissue culture flask containing 4 mL DMEM with 10% (v/v) FBS and 1% (v/v) pen-strep solution. The membranes were soaked with 75% alcohol overnight and UV-sterilized for 4 h, subsequently arranged in 24-well cell-culture plates at a density of 1×10^4 cells/well. Six replicates were used for each sample. Cell viability was measured using CCK-8 assays according to the manufacturers' instructions. Cell proliferation results are presented as optical density (OD) measured at 450 nm using an enzyme-linked immunosorbent assay plate reader (Multiskan MK3, Thermo electron corporation, USA). Three independent experiments were performed for each assay condition.

Acridine orange/ethidium bromide (AO/EB) double fluorescent dyes were used to qualitatively observe apoptotic cells. After stained with AO/EB, the cells immediately observed and photographed by an inverted fluorescence microscope (Olympus CKX41, Tokyo, Japan) equipped with an Olympus DP70 digital camera. Cells morphologies on different membrane surfaces after successively incubated with Rhodamine phalloidin (Molecular Probes, USA) and 4′, 6-diamidino-2-phenylindole (DAPI, Molecular Probes, USA) were observed by confocal laser scanning microscopy (CLSM; 510 Meta Duo Scan; Carl Zeiss, Germany).

Table 1
Surface elemental percentages of C, O and N of the membranes.

Samples	Elemental percentages (%)			Binding energy and relative area (%)					
	C	O	N	C—C (284.6 eV)	C—O (286.0 eV)	O=C—O (287.5 eV)	O—C—O (287.9 eV)	O=C—N (289.0 eV)	C/N (%)
PU	88.41	9.92	4.28	56.74	22.85	–	–	8.82	20.66
D-PU	75.13	16.50	4.77	39.62	18.16	11.60	–	5.75	15.75
C-D-PU	77.47	15.09	4.64	49.11	18.37	–	9.99	–	16.70

3. Results and discussion

3.1. Thermal stability and surface compositions of the PU, D-PU and C-D-PU membranes

Thermal stability of the PU, D-PU and C-D-PU membranes was studied by TGA, and corresponding TGA and DTG curves were shown in Fig. 2(A). Pure PU membrane decomposed in a third-stage pattern. The first one in range of 270–350 °C was ascribed to the degradation of hard segments of PU. Both the second stage (350–390 °C) and third stage (390–540 °C) should be related to the degradation of soft segments of PU, which is in agreement with the literature reported (Petrović, Zavargo, Flyn, 1994). The result suggested the complexity of the decomposition process. Compared with that of pure PU, D-PU and C-D-PU showed the similar thermal degradation patterns, but differences in thermal stability can be obviously observed. The onset temperature (T_{1on}) of the first stage increased from 271.1 °C to 295.2 °C and 295.5 °C, and the maximum decomposition temperature (T_{1max}) increased from 324.6 °C to 355.0 °C and 358.1 °C by coated PDOPA and COS onto PU membrane, respectively. The increase in thermal stability of D-PU and C-D-PU compared with pure PU may be reasonably ascribed to the formation of cross-linked PDOPA layer, most of which hardly decomposed during the TG process (Wang, Jiang, Wen, Liu, & Zhang, 2012). It is worth mentioning that size of the second peak of C-D-PU increased comparing with that of pure PU and D-PU, which may be due to the fact that both the decomposition of soft segments of PU and COS contributed to this stage. According to the literature reported, the maximum decomposition temperature of COS is about 302 °C (Kaya, Asan-Ozusaglam, & Erdogan, 2016). The increase in decomposition temperature of COS obtained in this study may be attributed to the increase in thermal stability of COS after reacted with PDOPA. Additionally, as shown in enlarged profile, the residual weight of D-PU membrane at 800 °C is about 8.0%, which is higher than that of C-D-PU (6.9%) and pure PU (5.3%) membranes. This could also be explained by the fact that the crosslinked main chain of PDOPA layer is hardly decomposed during the TG process (Liu et al., 2013; Wang et al., 2015).

The surface chemical composition of the PU, D-PU and C-D-PU membranes was analyzed by XPS. Wide scans and high-resolution C1 s peaks of XPS spectra of the membranes are given in Fig. 2(B), and typical percentage of functional groups calculated from the C1 s spectra is listed in Table 1. PU showed three peaks corresponding to C1 s (285 eV), O1 s (532 eV) and N1 s (400 eV) on wide scan XPS spectrum with a C/N content ratio of 20.66. The nitrogen content of PU membrane is higher than the values reported in literatures. One reason for this result is presumably due to differences in composition and structure of PU used in different reports. Another reason may be ascribed to a rearrangement of soft and hard segments of PU on membrane surface, which allows hydrophilic and polar urethane groups in hard segments relatively tend to expose on the membrane surface, thereby increasing the nitrogen content on the surface of PU. D-PU and C-D-PU membranes also show the three peaks of C1 s (285 eV), O1 s (532 eV) and N1 s (400 eV) on wide scan XPS spectra. But in contrast to PU, the C/N content ratio of D-PU and C-D-PU membranes decreased to 15.75 and 16.70, respectively. Moreover, the C/N content ratio of D-PU is slightly lower than that of C-D-PU, which is consistent with the nitrogen content in DOPA ($C_8H_9NO_2$, the nitrogen content is about 9.15%) and COS ($C_{12}H_{24}N_2O_9$, nitrogen content is about 8.23%).

Further observation indicated that C1 s core-level spectrum of PU membrane was deconvoluted into three peaks: C—C (284.6 eV, 56.74%), C—O (286.0 eV, 22.85%) and O=C—N (289.0 eV, 8.82%). The result is in consistent with literatures reported (Hsu & Chen, 2000; Zhu et al., 2011 Zhu, Jiang, Zhu, & Xu, 2011). After modified with PDOPA, there was a significant decrease in the three peaks of 284.6, 286.0 and 289.0 eV, as well as appearance of a new peak in 287.5 eV attributing to ketone (C=O) group of PDOPA layer (Postma et al., 2009). For C-D-PU membrane, a new peak at 287.9 eV attributing to O—C—O group of saccharide unit of COS can be observed (De Giglio, Trapani, Cafagna, Sabbatini, & Cometa, 2011). Moreover, the absence of both the peaks at 289.0 eV (relevant to O=C—N functionalities of PU) and 287.5 eV (corresponding to C=O group of PDOPA) suggested that dense COS layer has thoroughly covered through the whole surface of the membrane. According to the previous studies (Li et al., 2016; Mccloskey et al., 2010), the physically absorbed PDOPA, and water soluble DOPA and COS can be easily removed by washing with deionized water and ethanol. Thus, combining the results of TGA and XPS together, it can conclude that PDOPA and COS have been chemically immobilized on the surface of PU membrane, respectively.

3.2. Surface morphologies of the PU, D-PU and C-D-PU membranes

Surface morphologies of the PU, D-PU and C-D-PU membranes were observed by FESEM, and the images are shown in Fig. 3(A). Pure PU showed a dense and uniform surface with some "sea-island structure" due to microphase separation between soft and hard segments (Mondal, Hu, & Yong, 2006). The isolated microdomains most likely represent hard segments and continuous phase corresponds to soft segments of PU, respectively. Compared with pure PU, a rougher surface with obvious light and dark domains was observed on the surface of D-PU membrane, suggesting the formation of PDOPA layer. Moreover, an increase in thickness of PDOPA layer in isolated domains can be observed, which resulted in an

Table 2
Surface energy components of the PU, D-PU and C-D-PU membranes.

Samples	Contact angle (deg)		Surface-energy components (mJ/m^2)			
	Water	Diiodomethane	γ_S	γ_s^d	γ_s^p	$(\gamma_S - \gamma_{S0})/\gamma_{S0}$
PU	90.4 ± 4.3	67.8 ± 2.1	25.3 ± 0.6	20.8 ± 0.2	4.5 ± 0.1	–
D-PU	68.3 ± 1.4	56.3 ± 3.7	37.9 ± 0.5	23.4 ± 0.9	14.5 ± 0.2	0.50
C-D-PU	59.8 ± 1.2	53.0 ± 2.7	43.7 ± 0.9	23.7 ± 0.3	20.0 ± 0.7	0.73

Table 3
Quantitative analysis of *E. coli* and *S. aureus* and zeta potential (pH = 7) of the PU, D-PU and C-D-PU membranes.

Samples	Number of *E. coli* colonies (CFU/mL)	Number of *S. aureus* colonies (CFU/mL)	ABE of *E. coli* (%)	ABE of *S. aureus* (%)	Zeta potential (mV)
PU	1.36×10^7	1.64×10^7	–	–	−16.94
D-PU	1.24×10^7	1.46×10^7	8.82	10.98	−25.42
C-D-PU	8.78×10^6	8.40×10^6	35.44	48.78	34.38

increase in surface roughness of the membrane. The reason for this phenomenon is may be that DOPA tends to self-polymerization in isolated domains which with stronger polarity comparing to continuous phase, but more research is needed to better understand this phenomenon. Dissimilar to D-PU membrane, a relative uniform surface was obtained for the C-D-PU membrane after further immobilized with COS.

Surface topologies of the PU, D-PU and C-D-PU membranes were further observed using AFM, and the results are shown in Fig. 3(B). Pure PU membrane displayed a "sea-island structure" surface with the RMS value was 9.89 ± 0.3 nm based on 5.0 um × 5.0 um scan area. A more typical "sea-island structure" can be observed on the surface of D-PU membrane, and the RMS value of D-PU membrane correspondingly increased to 19.10 ± 0.7 nm, indicating the surface roughness of PU membrane obviously increased by coated with PDOPA layer. Compared with that of D-PU, a relative uniform surface with scaly structure can be seen on the C-D-PU membrane, and the RMS value decreased to 12.70 ± 0.6 nm but was still higher than that of pure PU. The AFM observation is in consistent with the result of FESEM. The changes in topologies and increase in surface roughness of the PU membrane by modified with PDOPA and COS will affect the adhesion and proliferation of cells and bacteria (Lampin, Warocquier-Clérout, Legris, Degrange, & Sigot-Luizard, 1997; Li et al., 2016).

3.3. Hydrophilicity and surface energy of the PU, D-PU and C-D-PU membranes

The contact angle (CA) of the PU, D-PU and C-D-PU membranes was measured using water and diiodomethane as probe liquids, and the result was shown in Table 2. PU membrane showed a relative high CA value of $90.4 \pm 4.3^\circ$ and $67.8 \pm 2.1^\circ$ against water and diiodomethane, respectively. The CA values against two above-mentioned liquids obtained for D-PU and C-D-PU membranes are considerably lower than those of pure PU, suggesting that the hydrophilicity of PU membrane was obviously improved by modified with PDOPA and COS. The reason for this phenomenon was possibly attributed to comprehensive influences of the hydrophilic characteristics of PDOPA and COS molecules, and changes in surface roughness after modification.

Surface energy is often used to evaluate surface wettability and hydrophilicity, the higher the surface energy, the better the surface hydrophilicity (Kozbial et al., 2014). In this study, Owens-Wendt model was used for determining surface energy from CA data, which allows for dissociation of total surface energy into polar and nonpolar components (Owens & Wendt, 1969). As shown in Table 2, the γ_S value of PU membrane increased from 25.3 ± 0.6 mJ/m^2 to 37.9 ± 0.5 and 43.7 ± 0.9 mJ/m^2 after surface modified with PDOPA and COS respectively, suggesting that the hydrophilicity of the membrane was improved. Moreover, the value of the $\gamma_s{}^p$ increased obviously, but the $\gamma_s{}^d$ changed little, which indicated that the polar component plays a major role in contributing to the increase of surface energy and hydrophilicity of the membranes.

Here, γ_S refers to the total surface energy of the membranes; $\gamma_s{}^d$ and $\gamma_s{}^p$ represent the dispersive component and polar component of the membranes, respectively; γ_{S0} refers to the total surface energy of pure PU membrane; $(\gamma_S - \gamma_{S0})/\gamma_{S0}$ refers to the change in γ_S of the modified PU membranes compared to that of pure PU membrane.

3.4. Antibacterial activity of the PU, D-PU and C-D-PU membranes

Antibacterial activity of the membranes was investigated against Gram negative bacteria *E. coli* and Gram positive bacteria *S. aureus* by spread plate test. As shown in Table 3, in contrast to PU membrane, the ABE value of *E. coli* and *S. aureus* on D-PU and C-D-PU membranes was 8.82% and 10.98%, and 35.44% and 48.78%,

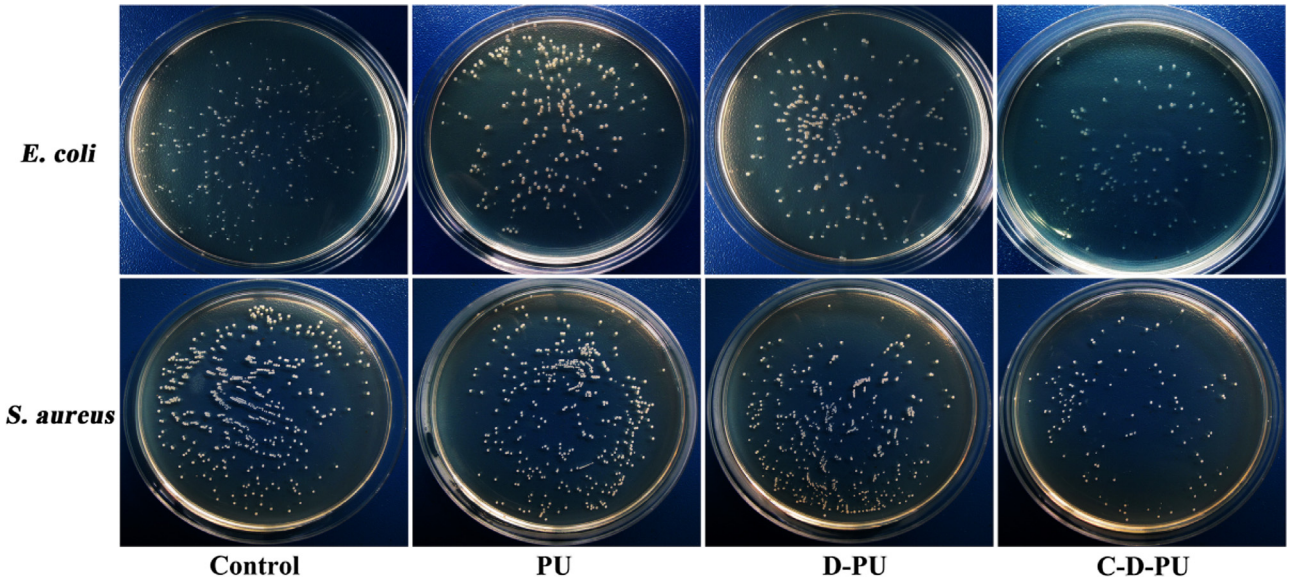

Fig. 4. Photographs of agar plates corresponding to *E. coli* and *S. aureus* on the membranes.

respectively. Fig. 4 showed the live bacteria on the membranes for 12 h incubation. It can be observed that the number of live bacteria slightly decreased on D-PU membrane and significantly decreased on C-D-PU membrane compared with PU membrane. The results suggested that the antibacterial activity of PU membrane weakly increased by modified with PDOPA, but significantly increased by further modified with COS.

The adhesion and multiplication of bacteria on material surfaces relate with many factors, including surface roughness, surface energy, surface charge and chemical composition. Generally, higher surface roughness also associates with increasing plaque accumulation. In this study, although surface roughness of D-PU and C-D-PU membranes is higher than that of pure PU membrane, the effect of surface roughness on bacterial adhesion and multiplication was possibly negligible since surface roughness of the pristine and modified PU membranes is less than 10 nm. In terms of surface energy, a higher surface energy is more prone to bacterial adherence and multiplication. Thus, the increase in surface energy of PU membrane by successively modified with PDOPA and COS may be resulted in the increase of bacterial adherence and multiplication. Last but the most important factors are surface charge and chemical composition. Generally, positively charged molecules can facilitate their binding with negative charge of bacterial cell wall to prevent the nutrition transport and lead to the inhibition of bacterial growth (Eaton, Fernandes, Pereira, Pintado, & Xavier Malcata, 2008; Helander, Nurmiaho-Lassila, Ahvenainen, Rhoades, & Roller, 2001). Both the increase and decrease in antibacterial activity by coating with PDOPA can be found in literatures (Iqbal, Lai, & Avis, 2012; Sileika, Kim, Maniak, & Messersmith, 2011). The zeta potential (pH = 7) of PU and D-PU membrane was −16.94 and −25.42 mV respectively, which are consistent with the relevant literature (Liu et al., 2015). Thus, the PU and D-PU membranes are slightly prone to the adhesion and multiplication of Gram positive bacteria *S. aureus* compared with Gram negative bacteria *E. coli*. As shown in Table 3, it is interesting that the antibacterial activity of positively charged C-D-PU (34.38 mV) is more efficient against Gram positive bacteria *S. aureus* than against Gram negative bacteria *E. coli*. The result is in consist with that reported in literature, which indicated that COS with lower molecular weight has better antibacterial efficacy against Gram positive bacteria compared with Gram negative bacteria (M. Jeon, Park, & Kim, 2001). Taking together, it can conclude that the changes in antibacterial activity of PU by coating with PDOPA and COS layers should be ascribed to the comprehensive influences of surface roughness, surface energy, surface charge and composition.

3.5. Proliferation and microstructures of cells on all membranes

The proliferation and viability of NIH-3T3 cells on PU, D-PU and C-D-PU membranes were evaluated by CCK-8 assay and OD values, and the result were shown in Fig. 5(A). The OD values of cells cultured on all the membranes increased slowly with time in the first four days, indicating the growth of NIH-3T3 cells in the lag phase. However, up to 7 days cultivation, the OD values of NIH-3T3 cells on all the membranes remarkably increased, suggesting cells growth has entered into a logarithmic phase. Moreover, the OD values of NIH-3T3 cells on the D-PU and C-D-PU membranes were significantly higher than those of cells on pure PU membrane, which suggested that PDOPA and COS layers can prompt the proliferation and viability of NIH-3T3 cells. More importantly, the OD values of NIH-3T3 cells on C-D-PU membrane are slightly higher than those of cells on D-PU membrane. This result is in consistent with reports in literatures, which revealed that both PDOPA and COS are in favor of the proliferation and viability of mouse embryo osteoblast precursor (MC3T3-E1) cells. The increase in the OD values of NIH-3T3 cells on the modified PU membranes may be mainly ascribed to

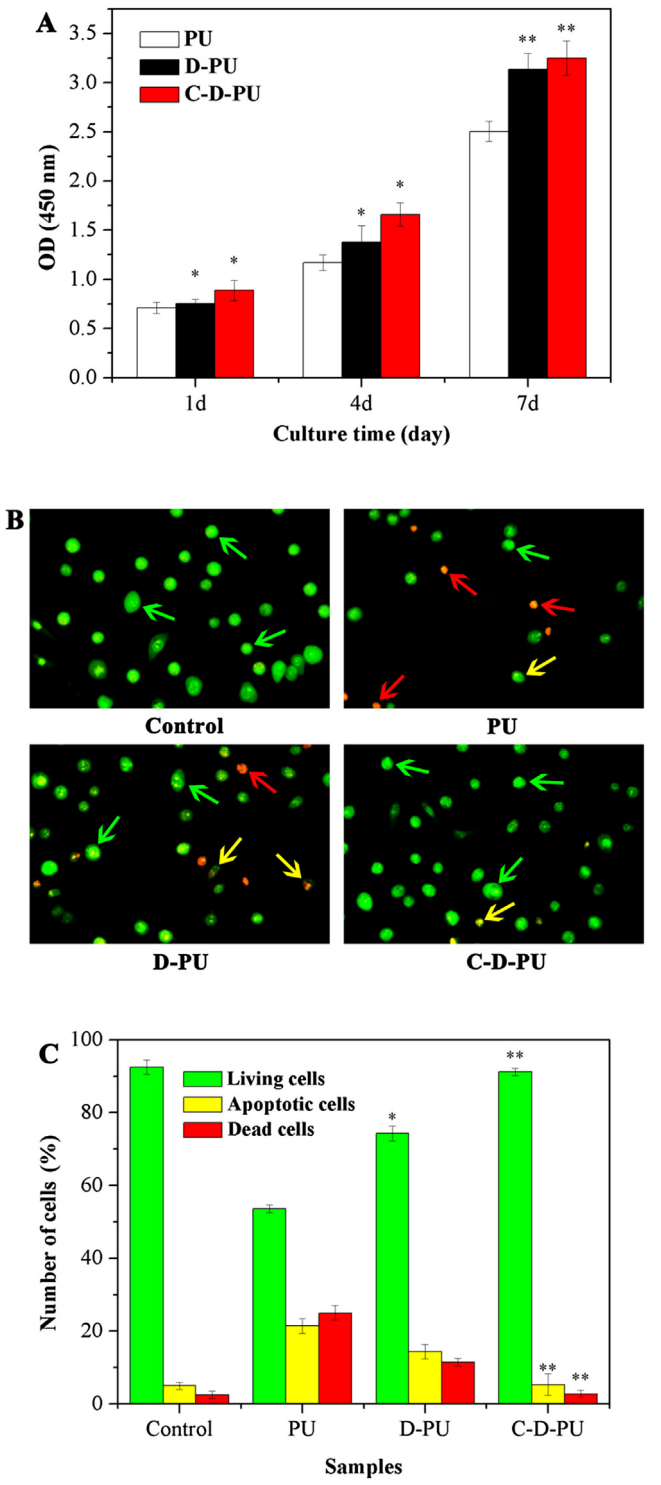

Fig. 5. (A) Proliferation of NIH-3T3 cells seeded on the membranes (Data presented as mean ± SD, $n = 5$, $^{*}P < 0.05$, $^{**}P < 0.01$ versus PU membrane group); (B) Fluorescene micrographs (magnification × 200) of NIH-3T3 cells stained with AO/EB for 24 h (Green arrow, living cells; orange arrow, apoptotic cells; red arrow, dead cells); (C) Quantification of AO/EB stained NIH-3T3 cells for 24 h on the membranes (Data presented as mean ± SD, $n = 3$, $^{*}P < 0.05$, $^{**}P < 0.01$ versus PU membrane group) (for interpretation of the references to colour in this figure legend, the reader is referred to the web version of this article).

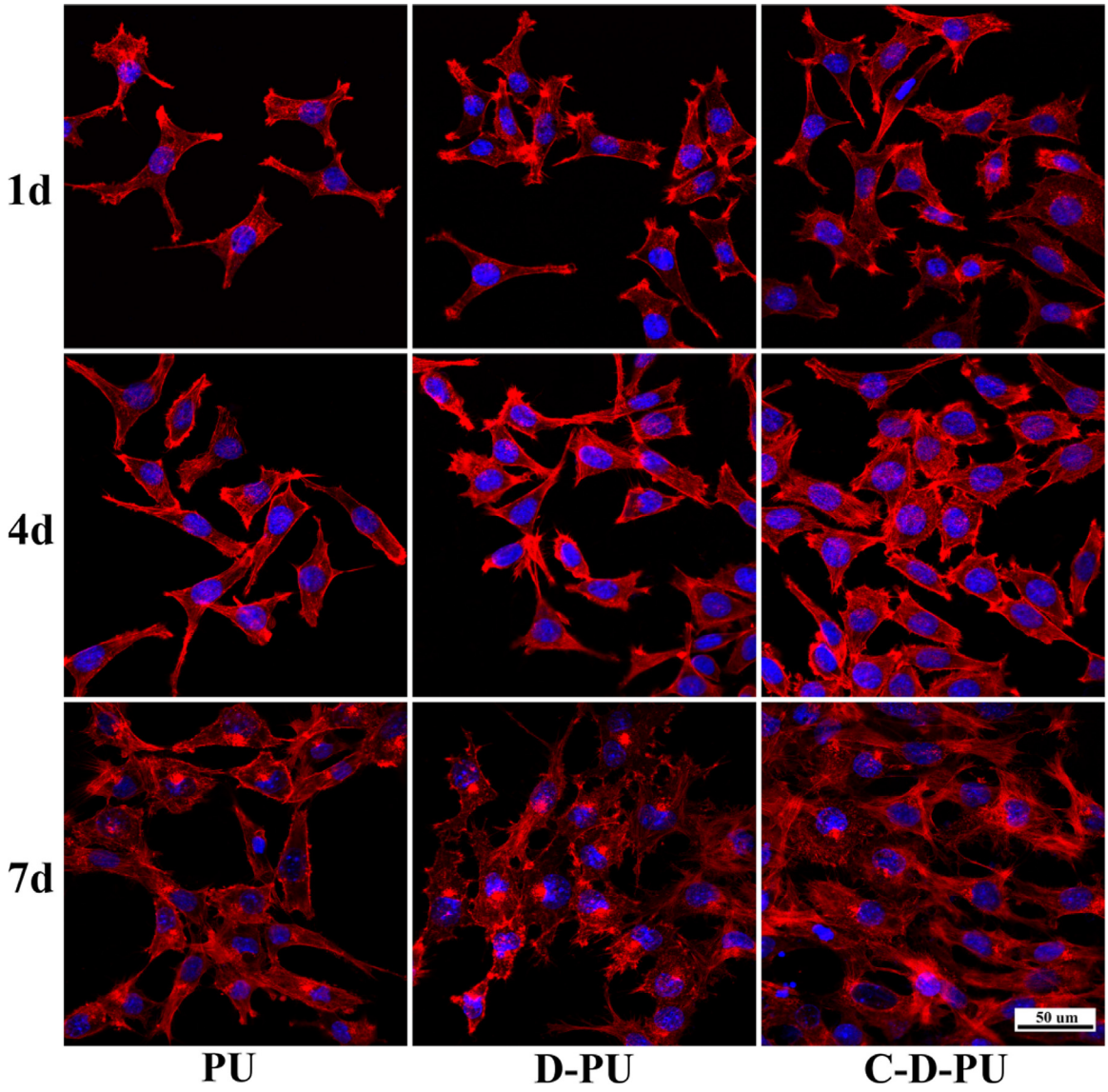

Fig. 6. CLSM images of NIH-3T3 cells growth on the membranes.

the relative high surface roughness and active hydroxyl, amine or imino groups on PDOPA and COS layers (Bacakova, Filova, Parizek, Ruml, & Svorcik, 2011; Becker et al., 2002).

The fluorescene micrographs of NIH-3T3 cells cultured on different membranes stained with AO/EB were shown in Fig. 5(B), and corresponding quantitative analysis on living (light green), apoptotic (light orange) and dead (light red) cells was given in Fig. 5(C) (Jeyaraj et al., 2013). AO/EB staining revealed that control cells exhibit normal morphological features with light green nucleus. While cells exposed to pure PU membrane, both apoptotic and dead cells with orange and red nuclei can be observed, respectively. For the D-PU membrane, the number of living cells increased, but there still were some apoptotic and dead cells. While cells exposed to the C-D-PU membrane showed a regular morphology with an increase in the number of living cells, which looked quite similar to those of the control group. It suggested that the COS layer on D-PU membrane can promote the attachment and proliferation of NIH-3T3 cells, and regulate the level of cell vitality. Fig. 5(C) showed quantitative data on the percentage of living, apoptotic and dead cells on the membranes. From the result, 53.6% living cells, 21.4% apoptotic cells and 25% dead cells were observed on PU membrane. Whereas, after modified with PDOPA, the percentage of living cells was increased to 74.3%, while apoptotic and dead cells were decreased to 14.3% and 11.4%, respectively. The maximum percentage of living cells was observed for those cultured on the C-D-PU membrane (91.2%), and the sum percentage of apoptotic cells and dead cells was less than 8%.

The cytoskeleton and nucleus of NIH-3T3 cells on the membranes were observed by CLSM (Fig. 6). For 1 day cultivation, almost all of NIH-3T3 cells showed spindle-like shapes, but there are significant differences in cell number, width and spreading area on different membranes. Cells cultured on PU displayed a narrow morphology with little protrusions. In contrast, cells on D-PU and C-D-PU membranes, particularly on the latter, showed a larger attachment and spreading area with some protrusions and increased number of cells. Prolong the cultivation, cells pseudopodia formed further, leading to rapid cell spreading and formation of bridge connections between adjacent cells on C-D-PU membrane. Up to 7 days cultivation, the adherent cells were evenly distributed and spread on the C-D-PU membrane with a stretched appearance, displaying irregular and polygonal morphologies with lots of pseudopodia, while those on pure PU membrane still nearly show a spindle-like morphology with less number of cells and cell spreading area. The result indicated that bioactive PDOPA and COS layers,

particularly the latter, can facilitate the attachment and spreading of NIH-3T3 cells.

4. Conclusions

In this work, a simple and effective surface modification approach for PU membrane was conducted. TGA and XPS measurements revealed that PDOPA and COS have been successively immobilized on the surface of PU membrane. The rougher surface created by PDOPA and COS enabled the PU membrane to possess higher surface energy and better hydrophilicity, which were more in favor of the attachment and proliferation of NIH-3T3 cells. In addition, the antibacterial activity of PU membrane slightly increased by modified with PDOPA, but significantly increased by modified with COS. As a consequence, the D-PU and C-D-PU membranes, especially the latter, are not only in favor of preserving moisture and accelerating wound healing but also can increase the antibacterial activity. Thus the resulting C-D-PU membrane can be expected to have potential applications as a wound dressing material.

Acknowledgements

This work was supported by the National Natural Science Foundation of China (31570981, 31571030 and 51473069), Guangdong Provincial Natural Science Foundation of China (2016A030313086), Project on the Integration of Industry, Education and Research of Guangdong Province (2013B090500107), Science and Technology Program of Guangzhou, China (No. 201510010135).

References

Bacakova, L., Filova, E., Parizek, M., Ruml, T., & Svorcik, V. (2011). Modulation of cell adhesion: Proliferation and differentiation on materials designed for body implants. *Biotechnology Advances*, *29*, 739–767.

Becker, D., Geißler, U., Hempel, U., Bierbaum, S., Scharnweber, D., Worch, H., & Wenzel, K. W. (2002). Proliferation and differentiation of rat calvarial osteoblasts on type I collagen-coated titanium alloy. *Journal of Biomedical Materials Research*, *59*, 516–527.

Chandika, P., Ko, S. C., Oh, G. W., Heo, S. Y., Nguyen, V. T., Jeon, Y. J., & Park, W. S. (2015). Fish collagen/alginate/chitooligosaccharides integrated scaffold for skin tissue regeneration application. *International Journal of Biological Macromolecules*, *81*, 504–513.

De Giglio, E., Trapani, A., Cafagna, D., Sabbatini, L., & Cometa, S. (2011). Dopamine-loaded chitosan nanoparticles: Formulation and analytical characterization. *Analytical and Bioanalytical Chemistry*, *400*, 1997–2002.

Eaton, P., Fernandes, J. C., Pereira, E., Pintado, M. E., & Xavier Malcata, F. (2008). Atomic force microscopy study of the antibacterial effects of chitosans on Escherichia coli and *Staphylococcus aureus*. *Ultramicroscopy*, *108*, 1128–1134.

Hashemi Doulabi, A., Mirzadeh, H., Imani, M., & Samadi, N. (2013). Chitosan/polyethylene glycol fumarate blend film: Physical and antibacterial properties. *Carbohydrate Polymers*, *92*, 48–56.

Helander, I. M., Nurmiaho-Lassila, E. L., Ahvenainen, R., Rhoades, J., & Roller, S. (2001). Chitosan disrupts the barrier properties of the outer membrane of gram-negative bacteria. *International Journal of Food Microbiology*, *71*, 235–244.

Hsu, S. H., & Chen, W. C. (2000). Improved cell adhesion by plasma-induced grafting of L-lactide onto polyurethane surface. *Biomaterials*, *21*, 359–367.

Hu, S. G., Jou, C. H., & Yang, M. C. (2003). Antibacterial and biodegradable properties of polyhydroxyalkanoates grafted with chitosan and chitooligosaccharides via ozone treatment. *Journal of Applied Polymer Science*, *88*, 2797–2803.

Iqbal, Z., Lai, E. P. C., & Avis, T. J. (2012). Antimicrobial effect of polydopamine coating on *Escherichia coli*. *Journal of Materials Chemistry*, *22*, 21608–21612.

Jeon, Y. J., Park, P. J., & Kim, S. K. (2001). Antimicrobial effect of chitooligosaccharides produced by bioreactor. *Carbohydrate Polymers*, *44*, 71–76.

Jeyaraj, M., Sathishkumar, G., Sivanandhan, G., Mubarakali, D., Rajesh, M., Arun, R., & Premkumar, K. (2013). Biogenic silver nanoparticles for cancer treatment: An experimental report. *Colloids & Surfaces B Biointerfaces*, *106*, 86–92.

Kaya, M., Asan-Ozusaglam, M., & Erdogan, S. (2016). Comparison of antimicrobial activities of newly obtained low molecular weight scorpion chitosan and medium molecular weight commercial chitosan. *Journal of Bioscience and Bioengineering*, *121*, 678–684.

Kozbial, A., Li, Z., Conaway, C., McGinley, R., Dhingra, S., Vahdat, V., & Li, L. (2014). Study on the surface energy of graphene by contact angle measurements. *Langmuir*, *30*, 8598–8606.

Lampin, M., Warocquier-Clérout, R., Legris, C., Degrange, M., & Sigot-Luizard, M. F. (1997). Correlation between substratum roughness and wettability, cell adhesion, and cell migration. *Journal of Biomedical Materials Research*, *36*, 99–108.

Lee, H., Dellatore, S. M., Miller, W. M., & Messersmith, P. B. (2007). Mussel-inspired surface chemistry for multifunctional coatings. *Science*, *318*, 426-.

Li, H., Luo, C., Luo, B., Wen, W., Wang, X., Ding, S., & Zhou, C. (2016). Enhancement of growth and osteogenic differentiation of MC3T3-E1 cells via facile surface functionalization of polylactide membrane with chitooligosaccharide based on polydopamine adhesive coating. *Applied Surface Science*, *360*, 858–865.

Liu, Q., Wang, N., Caro, J., & Huang, A. (2013). Bio-inspired polydopamine: A versatile and powerful platform for covalent synthesis of molecular sieve membranes. *Journal of the American Chemical Society*, *135*, 17679–17682.

Liu, Y., Ai, K., & Lu, L. (2014). Polydopamine and its derivative materials: Synthesis and promising applications in energy, environmental and biomedical fields. *Chemical Reviews*, *114*, 5057–5115.

Liu, M., Zhou, J., Yang, Y., Miao, Z., Yang, J., & Tan, J. (2015). Surface modification of zirconia with polydopamine to enhance fibroblast response and decrease bacterial activity in vitro: A potential technique for soft tissue engineering applications. *Colloids & Surfaces B Biointerfaces*, *136*, 74–83.

Lowe, A., Bills, J., Verma, R., Lavery, L., Davis, K., & Balkus, K. J., Jr. (2015). Electrospun nitric oxide releasing bandage with enhanced wound healing. *Acta Biomaterialia*, *13*, 121–130.

Mccloskey, B. D., Park, H. B., Hao, J., Rowe, B. W., Miller, D. J., Chun, B. J., & Freeman, B. D. (2010). Influence of polydopamine deposition conditions on pure water flux and foulant adhesion resistance of reverse osmosis, ultrafiltration and microfiltration membranes. *Polymer*, *51*, 3472–3485.

Mondal, S., Hu, J. L., & Yong, Z. (2006). Free volume and water vapor permeability of dense segmented polyurethane membrane. *Journal of Membrane Science*, *280*, 427–432.

Muzzarelli, R. A. A., & Muzzarelli, C. (2002). *Chitosan in pharmacy and chemistry*.

Owens, D. K., & Wendt, R. C. (1969). Estimation of the surface free energy of polymers. *Journal of Applied Polymer Science*, *13*, 1741–1747.

Petrović, Z., Zavargo, J. H., & Flyn, W. J. (1994). Thermal degradation of segmented polyurethanes. *Journal of Applied Polymer Science*, *51*, 1087–1095.

Postma, A., Yan, Y., Wang, Y., Zelikin, A. N., Tjipto, E., & Caruso, F. (2009). Self-polymerization of dopamine as a versatile and robust technique to prepare polymer capsules. *Chemistry of Materials*, *21*, 3042–3044.

Sileika, T. S., Kim, H. D., Maniak, P., & Messersmith, P. B. (2011). Antibacterial performance of polydopamine-modified polymer surfaces containing passive and active components. *Acs Applied Materials & Interfaces*, *3*, 4602–4610.

Sun, B. K., Siprashvili, Z., & Khavari, P. A. (2014). Advances in skin grafting and treatment of cutaneous wounds. *Science*, *346*, 941–945.

Unnithan, A. R., Gnanasekaran, G., Sathishkumar, Y., Lee, Y. S., & Kim, C. S. (2014). Electrospun antibacterial polyurethane-cellulose acetate-zein composite mats for wound dressing. *Carbohydrate Polymers*, *102*, 884–892.

Wang, W., Jiang, Y., Wen, S., Liu, L., & Zhang, L. (2012). Preparation and characterization of polystyrene/Ag core-shell microspheres – A bio-inspired poly(dopamine) approach. *Journal of Colloid and Interface Science*, *368*, 241–249.

Wang, J., Bai, H., Zhang, H., Zhao, L., Chen, H., & Li, Y. (2015). Anhydrous proton exchange membrane of sulfonated poly(ether ketone) enabled by polydopamine-modified silica nanoparticles. *Electrochimica Acta*, *152*, 443–455.

Woo, H.-D., Park, K.-T., Kim, E.-H., Heo, Y., Jeong, J.-H., Pyun, D.-G., & Son, T.-I. (2015). Preparation of UV-curable gelatin derivatives for drug immobilization on polyurethane foam: Development of wound dressing foam. *Macromolecular Research*, *23*, 994–1003.

Xia, G., Lang, X., Kong, M., Cheng, X., Liu, Y., Feng, C., & Chen, X. (2016). Surface fluid-swellable chitosan fiber as the wound dressing material. *Carbohydrate Polymers*, *136*, 860–866.

Xu, H., Chang, J., Chen, Y., Fan, H., & Shi, B. (2013). Asymmetric polyurethane membrane with inflammation-responsive antibacterial activity for potential wound dressing application. *Journal of Materials Science*, *48*, 6625–6639.

Yan, W., Zhang, C., Zhang, Q., & Ping, L. (2011). Composite electrospun nanomembranes of fish scale collagen peptides/chito-oligosaccharides: Antibacterial properties and potential for wound dressing. *International Journal of Nanomedicine*, *6*, 667–676.

Yang, Y., & Yu, B. (2014). Recent advances in the synthesis of chitooligosaccharides and congeners. *Tetrahedron*, *70*, 1023–1046.

Yao, C., Li, X., Neoh, K. G., Shi, Z., & Kang, E. T. (2008). Surface modification and antibacterial activity of electrospun polyurethane fibrous membranes with quaternary ammonium moieties. *Journal of Membrane Science*, *320*, 259–267.

You, Y., Park, W. H., Ko, B. M., & Min, B. M. (2004). Effects of PVA sponge containing chitooligosaccharide in the early stage of wound healing. *Journal of Materials Science Materials in Medicine*, *15*, 297–301.

Zhu, L. P., Jiang, J. H., Zhu, B. K., & Xu, Y. Y. (2011). Immobilization of bovine serum albumin onto porous polyethylene membranes using strongly attached polydopamine as a spacer. *Colloids & Surfaces B Biointerfaces*, *86*, 111–118.